



NRC Publications Archive Archives des publications du CNRC

Integrated analysis of whole building heat, air and moisture transfer Tariku, F.; Kumaran, M. K.; Fazio, P.

This publication could be one of several versions: author's original, accepted manuscript or the publisher's version. /
La version de cette publication peut être l'une des suivantes : la version prépublication de l'auteur, la version
acceptée du manuscrit ou la version de l'éditeur.

For the publisher's version, please access the DOI link below. / Pour consulter la version de l'éditeur, utilisez le lien
DOI ci-dessous.

Publisher's version / Version de l'éditeur:

<https://doi.org/10.1016/j.ijheatmasstransfer.2010.03.016>

International Journal of Heat and Mass Transfer, 53, pp. 3111-3120, 2010-05-01

NRC Publications Record / Notice d'Archives des publications de CNRC:

<https://nrc-publications.canada.ca/eng/view/object/?id=1f1d4a64-b069-4ac5-bcb9-2ecc6a2d430d>

<https://publications-cnrc.canada.ca/fra/voir/objet/?id=1f1d4a64-b069-4ac5-bcb9-2ecc6a2d430d>

Access and use of this website and the material on it are subject to the Terms and Conditions set forth at

<https://nrc-publications.canada.ca/eng/copyright>

READ THESE TERMS AND CONDITIONS CAREFULLY BEFORE USING THIS WEBSITE.

L'accès à ce site Web et l'utilisation de son contenu sont assujettis aux conditions présentées dans le site

<https://publications-cnrc.canada.ca/fra/droits>

LISEZ CES CONDITIONS ATTENTIVEMENT AVANT D'UTILISER CE SITE WEB.

Questions? Contact the NRC Publications Archive team at

PublicationsArchive-ArchivesPublications@nrc-cnrc.gc.ca. If you wish to email the authors directly, please see the
first page of the publication for their contact information.

Vous avez des questions? Nous pouvons vous aider. Pour communiquer directement avec un auteur, consultez la
première page de la revue dans laquelle son article a été publié afin de trouver ses coordonnées. Si vous n'arrivez
pas à les repérer, communiquez avec nous à PublicationsArchive-ArchivesPublications@nrc-cnrc.gc.ca.





Integrated analysis of whole building heat, air and moisture transfer

NRCC-53316

Tariku, F.; Kumaran, M.K.; Fazio, P.

May 2010

A version of this document is published in / Une version de ce document se trouve dans:
International Journal of Heat and Mass Transfer, 53, pp. 3111-3120, May 01,
2010, DOI: [10.1016/j.ijheatmasstransfer.2010.03.026](http://dx.doi.org/10.1016/j.ijheatmasstransfer.2010.03.026)

The material in this document is covered by the provisions of the Copyright Act, by Canadian laws, policies, regulations and international agreements. Such provisions serve to identify the information source and, in specific instances, to prohibit reproduction of materials without written permission. For more information visit <http://laws.justice.gc.ca/en/showtdm/cs/C-42>

Les renseignements dans ce document sont protégés par la Loi sur le droit d'auteur, par les lois, les politiques et les règlements du Canada et des accords internationaux. Ces dispositions permettent d'identifier la source de l'information et, dans certains cas, d'interdire la copie de documents sans permission écrite. Pour obtenir de plus amples renseignements : <http://lois.justice.gc.ca/fr/showtdm/cs/C-42>



National Research
Council Canada

Conseil national
de recherches Canada

Canada 

Integrated Analysis of Whole Building Heat, Air and Moisture Transfer

Fitsum Tariku¹

British Columbia Institute of Technology, 3700 Willingdon Ave., Burnaby,

British Columbia, Canada V5G 3H2

Kumar Kumaran

National Research Council, Institute for Research in Construction, 1200 Montreal rd., Ottawa,

Ontario, Canada, K1A 0R6

Paul Fazio

Concordia University, 1455 de Maisonneuve Blvd. West, Montreal,

Quebec, Canada, H3G 1M8

Abstract

There is a continuous dynamic heat, air and moisture (HAM) interaction between the indoor environment, building envelope and mechanical systems. In spite of these interdependences, the current indoor, building envelope and energy analysis tools are used independently. In this paper a holistic HAM model that integrates building envelope enclosures, indoor environment, HVAC systems, and indoor heat and moisture generation mechanisms, and solves simultaneously for the respective design parameters is developed. The model is benchmarked with internationally published test cases that require simultaneous prediction of indoor environmental conditions, building envelope moisture performance and energy efficiency of a building.

Keywords: whole building HAM analysis, hygrothermal modeling, energy efficiency, indoor environment, thermal comfort, building envelope performance

¹ Corresponding author, email: Fitsum_tariku@bcit.ca

NOMENCLATURE

A_c condensate surface area (m^2)	\dot{m}_m mass flow rate of dry air (humidification/dehumidification systems) (kg/s)
A_i surface area of surface i (m^2)	\dot{m}_h mass flow rate of dry air (heating/cooling systems) (kg/s)
A_e evaporative surface area (m^2)	M molecular mass of water molecule (0.01806 kg/mol)
Cv_m specific capacity of solid matrix (J/(K·kg))	p zone vapour pressure (Pa)
Cp_a specific capacity of air (J/(K·kg))	P_{atm} atmospheric pressure (Pa)
Cp_v specific capacity of water vapor (J/(K·kg))	P_v vapour pressure (Pa)
D_l liquid conductivity (s)	\hat{P} saturated vapor pressure (Pa)
f_{sa} solar air factor (-)	p_i^s surface vapor pressure of surface i (Pa)
\bar{g} acceleration due to gravity (m/s^2)	\hat{p}_e saturated vapor pressure of reservoir e (Pa)
h_i^m mass transfer coefficient of surface i ($kg/(Pa \cdot s \cdot m^2)$)	\hat{p}_c saturated vapor pressure of condensate c (Pa)
h_i^h heat transfer coefficient of surface i ($W/(K \cdot m^2)$)	\dot{Q}_s heat source (W/m^3)
h_c^m mass transfer coefficient for condensate surface ($kg/(Pa \cdot s \cdot m^2)$)	R universal gas constant (8.314 J/mol)
h_e^m mass transfer coefficient for evaporation surface ($kg/(Pa \cdot s \cdot m^2)$)	T temperature ($^{\circ}C$)
h_{fg} latent heat of evaporation/condensation (J/kg)	T_e outdoor air temperature ($^{\circ}C$)
h_o outdoor surface heat transfer coefficient ($W/(K \cdot m^2)$)	T_i^s surface temperature of surface i ($^{\circ}C$)
I_o incident solar radiation (W/m^2)	\tilde{T} set point temperature ($^{\circ}C$)
I_t transmitted solar radiation (W/m^2)	U overall heat transfer coefficient ($W/(K \cdot m^2)$)
k_a air flow coefficient (s)	\bar{u} air velocity (m/s)
\dot{m} mass flow rate of dry air (kg/s)	\tilde{V} volume of the zone (m^3)
	w moisture content (kg/m^3)
	Y_a mass fraction of air (-)

Y_l mass fraction of liquid water (-)	μ air dynamic viscosity (kg/(m.s))
<u>Greek letters</u>	τ solar transmittance (-)
α solar absorptance (-)	ω humidity ratio (kg/kg dry air)
ϕ relative humidity (-)	ω_e humidity ratio of outdoor air (kg/kg dry air)
ρ_a density of air (kg/m ³)	ω_i^s humidity ratio of surface i (kg/kg dry air)
ρ_w density of water (kg/m ³)	$\tilde{\omega}$ set point humidity ratio (kg/kg dry air)
ρ_m density of material (kg/m ³)	δ_v vapor permeability (s).
λ_{eff} effective thermal conductivity (W/(m.K))	Θ sorption capacity (kg/m ³)

1 INTRODUCTION

Buildings are designed to create an isolated space from the surrounding environment and provide the desired interior environmental conditions for the occupants. In addition to fulfilling the function of creating favorable indoor environmental conditions, buildings are expected to be durable and energy efficient. These three functional requirements of the building should be optimized for a given climatic condition. This optimization process is necessary: 1) to provide a comfortable indoor environment to occupants since people spend most of their time indoors and their productivity is also dependent on how they perceive their indoor environment; 2) due to the high level of investment and maintenance costs² involved in the construction of new buildings and repair of building failures; 3) due to high energy consumption of buildings that results in high energy bills to maintain the desired building operating conditions.

Of course, exclusively dealing with one aspect of the building might lead to problems or yield less efficiency in the other aspects. For example, in early 1970's as a means of reducing energy consumption buildings were constructed and retrofitted to be more airtight and more highly insulated. Although the energy efficiency of the buildings improved, this new strategy created more problems in respect to durability of the building envelope due to high moisture accumulation in the building structure. The indoor humidity levels were also elevated due to the reduced air exchange, which resulted in low occupant comfort and health problems [1, 2].

To maintain the indoor humidity level within the design range, the building engineer needs to use an indoor model to evaluate different ventilation strategies and/or moisture

² According to Statistic Canada, over \$82 billion is invested in new building construction and about \$37 billion was spent for renovation in 2007 (http://www41.statcan.ca/2008/2162/ceb2162_000-eng.htm).

buffering materials, and decide on the appropriate material and equipment size for ventilation, humidification and dehumidification. However, the success of the strategy might depend on the robustness of the indoor model used to predict the indoor conditions. Most of the humidity models [3-6] ignore or lack comprehensive analysis of moisture exchange between the various building envelope components and the indoor air, despite the fact that approximately one-third of the moisture generated inside a room may be absorbed by moisture buffering materials [7,8]. In a reverse moisture exchange process, a significant amount of moisture is released to the indoor air from the building enclosure (e.g. initial moisture content of concrete) or/and surroundings through foundation walls, floor and above ground components [9]. This direct interaction of indoor air and building enclosure implies that to predict the indoor air-condition more accurately, the indoor model needs to be dynamically coupled with the building envelope model to capture the dynamic moisture and heat exchange between the construction and indoor air. Conversely, to realistically assess the hygrothermal performance of building envelope components the indoor boundary conditions need to be well known, contrary to the current practice of using predetermined simplistic or empirically generated conditions [10-14]. In reality the indoor conditions are determined by performing an integrated analysis of heat and mass balance of the external and internal loading as well as the mechanical systems' outputs. Energy models usually ignore the moisture effect on the thermal transport and storage properties of materials [15] as well as the local heating and cooling effects that are generated within the structure due to moisture phase changes (condensation and evaporation, respectively), which consequently affects the sensible and latent heat load calculations for the building. Incorrect prediction of the indoor air condition and ignoring moisture in the energy calculation might lead to an incorrect prediction of the required ventilation rate, energy demand for heating/cooling, as well as

humidification/dehumidification needed to maintain the intended building operating conditions. To deal with these interrelated and coupled effects, an integrated and fully coupled modeling approach that integrates the dynamic HAM transfer of the building envelope with the indoor environment and its components (i.e. HVAC system, moisture and heat sources) is necessary. In this paper, the development and benchmarking of a whole building hygrothermal model is presented. The model can be used to simultaneously assess building enclosure durability, indoor conditions, occupant comfort, and also the energy efficiency of a building with the objective of attaining efficient building design. The development and benchmarking of a building envelope model, which is an essential building block to the holistic HAM model described in this paper, is presented in Tariku et al[16] and Tariku [17].

2 WHOLE BUILDING HYGROTHERMAL MODEL DEVELOPMENT

The holistic HAM model that is developed in this paper considers the building as an integrated system consisting of building enclosure, indoor environment, mechanical systems, and the possible hygrothermal loadings. Figure 1 shows the schematic representations of the hygrothermal loadings that are expected in a typical building. The building is exposed to the local weather conditions including wind-driven rain and solar radiation on the outside, internal heat and moisture generations as well as solar gain on the inside. The building is also subjected to additional hygrothermal loadings related to mechanical systems for heating/cooling, de/humidification as well as ventilation.

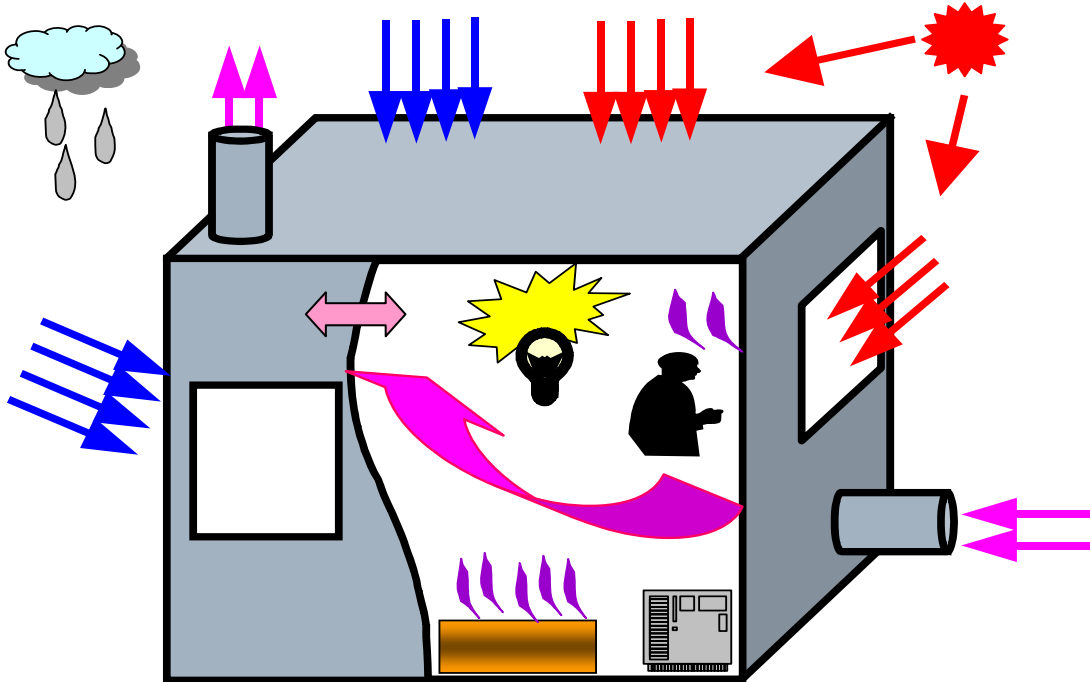


Figure 1 Typical hygrothermal loadings on a building.

Generally, the indoor environmental conditions, more specifically, temperature and relative humidity, are unknown quantities, and have to be determined from the heat and mass balance at the zone considering the three heat and moisture exchange mechanisms: 1) heat and mass transfer across the building enclosure; 2) internal heat and moisture generated by occupants and their activities, as well as; 3) heat and moisture supply by mechanical systems (heating, cooling, humidification, dehumidification and ventilation) depending on the mode of operation of the building.

In this paper, two primary models, namely the building envelope model and the indoor model, are integrated to form a whole building hygrothermal model. These primary models account for the three heat and moisture exchange mechanisms mentioned above. The building envelope model handles the heat and moisture exchanges between building enclosure and indoor

air, as well as the effect of the outdoor climatic conditions on the indoor environment and building envelope components' performance. The second and third heat and moisture transfer mechanisms, i.e. the internal heat and moisture generations and the mechanical systems outputs, are handled in the indoor model. In this section (2.1 to 2.3), the mathematical models that are implemented in the building envelope and indoor models as well as the integration of the two primary models are discussed. In the next section (3.1 to 3.3), the accuracy of the holistic HAM model is verified based on a comparison with results derived from internationally published benchmark exercises.

2.1 Building envelope model

A brief description of the transient building envelope model is presented, a detailed description of which are given in Tariku et al. [16] and Tariku [17]. The model has the capability of handling the non-linear and coupled HAM transfer through multilayered porous media by taking into account the non-linear hygrothermal properties of materials, moisture transfer by vapor diffusion, capillary liquid water transport and convective heat and moisture transfers. Moreover, the model accounts for the effect of moisture in the thermal storage and transfer properties of materials as well as the local heating and cooling effects that are generated within the structure due to moisture phase changes (i.e. condensation and evaporation, respectively). The partial differential equations (PDEs) that are implemented in the building envelope model are the following:

2.1.1 Moisture balance:

$$\Theta \frac{\partial \phi}{\partial t} = \nabla \cdot (D_\phi \nabla \phi + D_T \nabla T) - \nabla \cdot (D_l \rho_w \bar{g} + \rho_a \bar{u} C_c \hat{P} \phi) \quad (1)$$

$$\text{where } D_\phi = \left(\delta_v \hat{P} + D_l \frac{\rho_w R T}{M \phi} \right), \quad D_T = \left(\delta_v \phi \frac{\partial \hat{P}}{\partial T} + D_l \frac{\rho_w R}{M} \ln(\phi) \right) \text{ and } C_c = \frac{0.622}{P_{atm}}$$

2.1.2 Heat balance:

$$\begin{aligned} \rho_m C_{p_{eff}} \frac{\partial T}{\partial t} + \nabla \cdot (\bar{u} T) \rho_a (C_{p_a} + \omega C_{p_v}) + \\ \nabla \cdot (-\lambda_{eff} \nabla T) = \dot{m}_c h_{fg} + \dot{m}_c T (C_{p_v} - C_{p_l}) + \dot{Q}_s \end{aligned} \quad (2)$$

$$\text{where } C_{p_{eff}} = C_{v_m} + Y_a (C_{p_a} + \omega C_{p_v}) + Y_l C_{p_l} \text{ and } \dot{m}_c = \nabla \cdot (\delta_v \nabla P_v) - \rho_a \nabla \cdot (\bar{u} \omega)$$

2.1.3 Momentum balance (Darcy flow):

$$-\nabla \cdot \left(\rho_a \frac{k_a}{\mu} \nabla P \right) = 0 \quad (3)$$

The driving potentials of moisture and heat balance equations (Equation (1) and (2), respectively) are relative humidity and temperature, respectively. The airflow through the porous media is governed by the Darcy equation that relates the flow rate with pressure gradient and air

permeability characteristics of the media (Equation (3)). These nonlinear and coupled PDEs are solved simultaneously for temperature, moisture and airflow velocity fields across the computational domain (multi-layered building envelope component).

2.2 Indoor model

The indoor model was developed to predict the indoor temperature and humidity conditions based on the heat and moisture balance in the zone. The model accounts for the internal heat and moisture generation, mechanical systems outputs as well as the heat and moisture fluxes that cross the zone boundaries. The basic assumption of the model is that the indoor air is well mixed and can be represented by a single node. Based on this assumption, the indoor humidity and energy balance equations for a zone are derived as presented below.

2.2.1 *Indoor humidity balance*

The humidity balance equation incorporates the moisture absorption and desorption of the hygroscopic internal lining of building envelope components and furniture (\dot{Q}_b^m), moisture supply and removal from the zone by airflow (\dot{Q}_v^m), moisture addition and removal (humidification and dehumidification) by mechanical systems (\dot{Q}_m^m), moisture addition into the zone due to occupant activities (\dot{Q}_o^m), evaporation from a water reservoir (\dot{Q}_e^m), moisture removal due to moisture condensation on surfaces (\dot{Q}_c^m), and moisture removal by air-conditioning system (\dot{Q}_{ac}^m). Mathematically, the indoor humidity balance equation is represented by Equation (4).

$$\rho_a \tilde{V} \frac{d\omega}{dt} = \dot{Q}_b^m + \dot{Q}_v^m + \dot{Q}_m^m + \dot{Q}_o^m + \dot{Q}_e^m + \dot{Q}_c^m + \dot{Q}_{ac}^m \quad (4)$$

where:

$$\dot{Q}_b^m = \sum_i A_i h_i^m (p_i^s - p); \quad \dot{Q}_v^m = \dot{m}(\omega_e - \omega);$$

$$\dot{Q}_m^m = \dot{m}_m (\tilde{\omega} - \omega) \leq \dot{Q}_{m_max}^m;$$

$$\dot{Q}_e^m = \sum_e A_e h_e^m (\hat{p}_e - p); \quad \dot{Q}_c^m = C_c \cdot \sum_c A_c h_c^m (\hat{\omega}_c - \omega); \quad C_c = \frac{P_{atm}}{0.622}$$

The term $\dot{Q}_{m_max}^m$ is the maximum moisture supply or removal capacity of the humidification or dehumidification systems, respectively. Substituting these terms into the general humidity balance equation (Equation (4)), and rewriting vapor pressure in terms of humidity ratio yields Equation (5) for the case where the humidification/dehumidification demand is less than the equipment capacity ($\dot{Q}_m^m < \dot{Q}_{m_max}^m$).

$$\rho_a \tilde{V} \frac{d\omega}{dt} = -\omega \left(z \left[\sum_i A_i h_i^m + \sum_e A_e h_e^m + \sum_c A_c h_c^m \right] + \dot{m} + \dot{m}_m \right) + \left(z \left[\sum_i A_i h_i^m \omega_i^s + \sum_e A_e h_e^m \hat{\omega}_e + \sum_c A_c h_c^m \hat{\omega}_c \right] + \dot{m}\omega_e + \dot{m}_m \tilde{\omega} + \dot{Q}_o^m + \dot{Q}_{ac}^m \right) \quad (5)$$

and Equation (6) for the case where the demand is higher than the equipment capacity ($\dot{Q}_m^m \geq \dot{Q}_{m_max}^m$)

$$\rho_a \tilde{V} \frac{d\omega}{dt} = -\omega \left(z \left[\sum_i A_i h_i^m + \sum_e A_e h_e^m + \sum_c A_c h_c^m \right] + \dot{m} \right) + \left(z \left[\sum_i A_i h_i^m \omega_i^s + \sum_e A_e h_e^m \hat{\omega}_e + \sum_c A_c h_c^m \hat{\omega}_c \right] + \dot{m}\omega_e + \dot{Q}_{m_max}^m + \dot{Q}_o^m + \dot{Q}_{ac}^m \right)$$

2.2.2 Indoor energy balance

The general energy balance equation for the indoor air considers the energy exchange between the building envelope internal surfaces and the indoor air (\dot{Q}_b^h), the energy carried by the air flow into and out of the zone (\dot{Q}_v^h), the heat supply and removal (heating/cooling) by mechanical systems to maintain the room in the desired temperature range (\dot{Q}_m^h), the internal heat generated due to occupant activities (e.g. cooking) and building operation (e.g. lighting) (\dot{Q}_o^h), the energy supplied and removed from the interior space due to enthalpy transfer by moisture movement (\dot{Q}_h^h), and heat gain through the fenestration system (\dot{Q}_f^h). The contribution of each term in the total energy balance equation is described below. For the purpose of energy balance, the indoor air is assumed to be a mixture of dry air and water vapor only. Hence, the indoor energy balance in terms of mixture enthalpy is given by Equation(7).

$$\rho_a \tilde{V} \frac{dh}{dt} = \dot{Q}_b^h + \dot{Q}_v^h + \dot{Q}_m^h + \dot{Q}_o^h + \dot{Q}_h^h + \dot{Q}_f^h \quad (7)$$

$$\text{where: } \dot{Q}_b^h = \sum_i A_i h_i^h (T_i^s - T); \quad \dot{Q}_v^h = \dot{m} C p_a (T_e - T);$$

$$\dot{Q}_m^h = \dot{m}_h (C p_a + \omega C p_v) (\tilde{T} - T) \leq \dot{Q}_{m_max}^h;$$

$$\begin{aligned} \dot{Q}_h^h = & \underbrace{\dot{Q}_b^m C p_v T^{b*} + \dot{m} C p_v (\omega_e T_e - \omega T) + \dot{Q}_m^m C p_v T^{m*} + \dot{Q}_o^m C p_v T^o + \dot{Q}_e^m C p_v T^e + \dot{Q}_c^m C p_v T +}_{\text{Sensible heat}} \\ & \underbrace{h_{fg} (\dot{Q}_b^m + \dot{m} (\omega_e - \omega) + \dot{Q}_m^m + \dot{Q}_o^m + \dot{Q}_e^m + \dot{Q}_c^m + \dot{Q}_{ac}^m)}_{\text{Latent heat}} \end{aligned} ;$$

$$\dot{Q}_f^h = A_w \cdot \left(\underbrace{U(T_e - T)}_{\text{due to temperature difference}} + \underbrace{\frac{U}{h_o} \alpha I_o}_{\text{fraction of absorbed solar radiation}} + \underbrace{f_{sa} \tau I_o}_{\text{fraction of transmitted solar radiation}} \right)$$

For moisture absorption by building envelope surface T^{b*} is the indoor temperature; for desorption T^{b*} is the building envelope surface temperature. For humidification process T^{m*} is the temperature of the moisture releases by the equipment, and for dehumidification T^{m*} is the indoor air temperature T . T^o is the temperature of the moisture released by the indoor moisture source and T^e is the temperature of evaporating moisture. The term $\dot{Q}_{m_max}^h$ is the maximum sensible heating and cooling available from the respective equipment.

The term \dot{Q}_h^h accounts for the sensible and latent heat transfer that are generated due to moisture movement by ventilation (\dot{Q}_v^m) and convection at the building envelope surfaces (\dot{Q}_b^m); moisture gain or removal from the indoor space by mechanical systems (humidification/dehumidification) (\dot{Q}_m^m), and also other means: occupant activity (\dot{Q}_o^m), evaporation (\dot{Q}_e^m) and condensation (\dot{Q}_c^m), and \dot{Q}_{ac}^m is the moisture removal by air-conditioning system. This term along with the available latent and sensible heat capacities of the air-conditioning system can be estimated using latent degradation model [18,19]. The instantaneous heat gain to the indoor air through fenestration (\dot{Q}_f^h) is the sum of heat flow through the fenestration and a fraction of transmitted solar radiation ($f_{sa} I_t = f_{sa} \tau I_o$) which instantly heats the indoor air.

According to the European Standard pEN ISO 13791 [20]. the fraction of transmitted solar radiation that will be available as an immediate energy input to the indoor air ($f_{sa}I_t$) depends on the presence and quantity of very low thermal capacity items such as, carpets and furniture inside the room. The suggested values for the solar to air factor (f_{sa}) are 0, 0.1 and 0.2, for no furniture, a small amount of furniture, and a large amount of furniture, respectively. The rest of the transmitted radiation is assumed to be absorbed by the interior surfaces that later transfer part of the heat to the indoor air by convection. The radiation is assumed to be distributed uniformly in the indoor space, and each interior surface receives solar heat gain proportional to its surface area. Following mathematical manipulation of Equation (7), after substituting these terms, gives the final form of the indoor energy balance equation, Equation (8) for the case where the heating/cooling demand is less than the equipment capacity ($\dot{Q}_m^h < \dot{Q}_{m_max}^h$)

$$\rho_a \tilde{V} h_s \frac{dT}{dt} = -T \left(\sum_i A_i h_i^h + \dot{m} C p_a + \dot{m}_h h_s + U A_w + \dot{m} \omega_e C p_v + \dot{Q}_c^m C p_v \right) + \left(\sum_i A_i h_i^h T_i^s + \dot{m} C p_a T_e + \dot{m}_h h_s \tilde{T} + A_w \left(U T_e + \frac{U}{h_o} \alpha I_o + f_{sa} \tau I_o \right) + \dot{m} \omega_e C p_v T_e + \left(\dot{Q}_b^m C p_v T^{b*} + \dot{Q}_m^m C p_v T^{m*} + \dot{Q}_o^m C p_v T^o + \dot{Q}_e^m C p_v T^e \right) \right) \quad (8)$$

where $h_s = C p_a + \omega C p_v$ (sensible heat of the air-water vapor mixture)

and Equation (9) for the case where the demand is higher than the equipment capacity

$$\left(\dot{Q}_m^h \geq \dot{Q}_{m_max}^h \right)$$

$$\rho_a \tilde{V} h_s \frac{dT}{dt} = -T \left(\sum_i A_i h_i^h + \dot{m} C p_a + U A_w + \dot{m} \omega_e C p_v + \dot{Q}_c^m C p_v \right) + \left(\sum_i A_i h_i^h T_i^s + \dot{m} C p_a T_e + \dot{Q}_{m_max}^h + A_w \left(U T_e + \frac{U}{h_o} \alpha I_o + f_{sa} \tau I_o \right) + \dot{m} \omega_e C p_v T_e + \dot{Q}_b^m C p_v T^{b*} + \dot{Q}_m^m C p_v T^{m*} + \dot{Q}_o^m C p_v T^o + \dot{Q}_e^m C p_v T^e \right) \quad (9)$$

The moisture and heat addition into the zone due to occupant activities (\dot{Q}_o^m and \dot{Q}_o^h) are usually independent of the indoor condition, but rather on the occupant behavior. To reflect the level of occupants activities at various times, diurnal moisture and heat generation schedule are used in the indoor humidity and energy calculations.

2.3 Integration of building envelope and indoor models: Whole building

hygrothermal model

In the previous sections, the governing equations for HAM transport through building enclosure (Equation (1), (2) and (3)), and the indoor heat and moisture balance equations (Equation (5) and (7)) were stated. Integration of these equations in a single platform forms the basis of the whole building hygrothermal model. The heat and moisture balance equations of the building enclosure are coupled with the corresponding indoor heat and moisture balance equations through the hygrothermal conditions (temperature and relative humidity) of the interior surfaces. Consequently, during solving these coupled equations, a solution with interior surfaces' temperatures and relative humidity that satisfies both the building enclosure and indoor model equations is sought.

A graphical representation of the whole building hygrothermal model is shown in Figure 2. The hygrothermal responses of a building (indoor temperature and relative humidity, energy

consumption and building enclosure hygrothermal conditions) are the consequences of the dynamic interactions of various elements shown in Figure 2. The building enclosure may constitute many layers of different thickness, which may have unique non-linear hygrothermal properties. A change in the building enclosure design, say painting the interior surface or addition of insulation, or changes in climatic conditions will affect the indoor air conditions, which in turn affect the HVAC system outputs, say dehumidification or heating demand. Likewise, a change in the indoor heat and moisture generations or HVAC system output affects the indoor air conditions, which in turn affect the hygrothermal performance of the building enclosure. The holistic HAM model deals with these interrelated and coupled effects in a single platform, and simultaneously predicts the indoor temperature and relative humidity conditions, the moisture and temperature distributions in the building envelope components, as well as the heating and cooling loads.

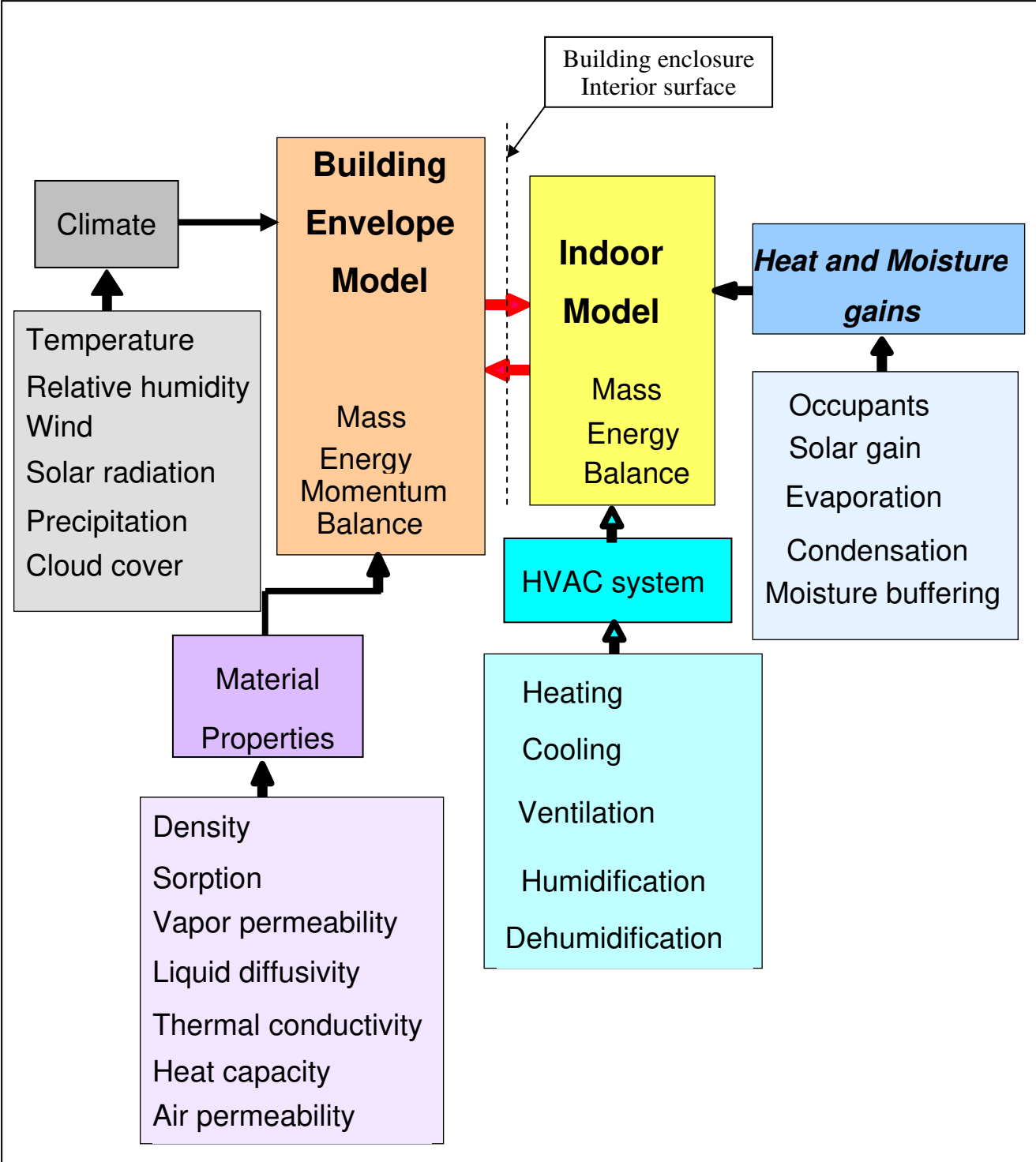


Figure 2 Schematic diagram of the whole building hygrothermal model.

The whole building hygrothermal model was developed on SimuLink simulation environment, which provides a smooth interface with the COMSOL Multiphysics³ and MatLab⁴ computational tools. The simulation environment allows full integration and dynamic coupling of the building envelope and indoor models.

Figure 3 shows the virtual simulation environment of a building that may be subjected to the hygrothermal loadings that are shown in Figure 1. The model takes into account the general specifications of the building including building location (i.e. latitude, longitude, altitude), topography (terrain roughness—is the building located in an open flat land or in dense urban area) and surrounding environment (degree of obstacles around the building) that may affect wind pressure and air infiltration calculations, building size and orientation, surface area of the building envelope components, orientation, and the component inclination and air tightness. The six building envelope components (four walls, roof and floor) are encapsulated in the “Zone Enclosure” block shown in Figure 3. The building components can be composed of different layers of materials and thickness, and can also be exposed to different exterior boundary conditions. The block subtitled “Mechanical Systems and Indoor heat and moisture gains” consists of mechanical systems for heating/cooling, humidification/dehumidification, ventilation, and indoor moisture and heat generations. The indoor “Furniture” block plays an important role in regulating the indoor humidity condition of the house. In the holistic HAM model it is represented as an interior building envelope component whose exterior surfaces are exposed to the indoor environmental conditions. The outputs of the “Window” block, which are the heat flux and window condensation rate, can significantly influence the indoor environmental conditions. The specifications of the windows on the four orientations can be different. The

³ COMSOL Multiphysics: <http://www.comsol.com/>

⁴ Mathworks <http://www.mathworks.com>

internal heat and moisture sources that can be represented as a lumped system (for example, evaporation of water from a sink or cooling of hot pan) are represented by the “Internal Heat and Moisture source/sink-Lumped system” block. Finally, the outputs of all the blocks are passed to the “Zone Humidity and Energy balance” block, where the two linear first-order differential equations for heat and moisture balances (Equation (5) and (7), respectively) are solved for the indoor temperature and humidity ratio. The outputs of the holistic HAM model include: 1) transient temperature and moisture distribution across each building envelope component; 2) transient indoor temperature and relative humidity conditions, and; 3) transient heating and cooling loads. In the next section, the whole building hygrothermal model is benchmarked against internationally published test cases.

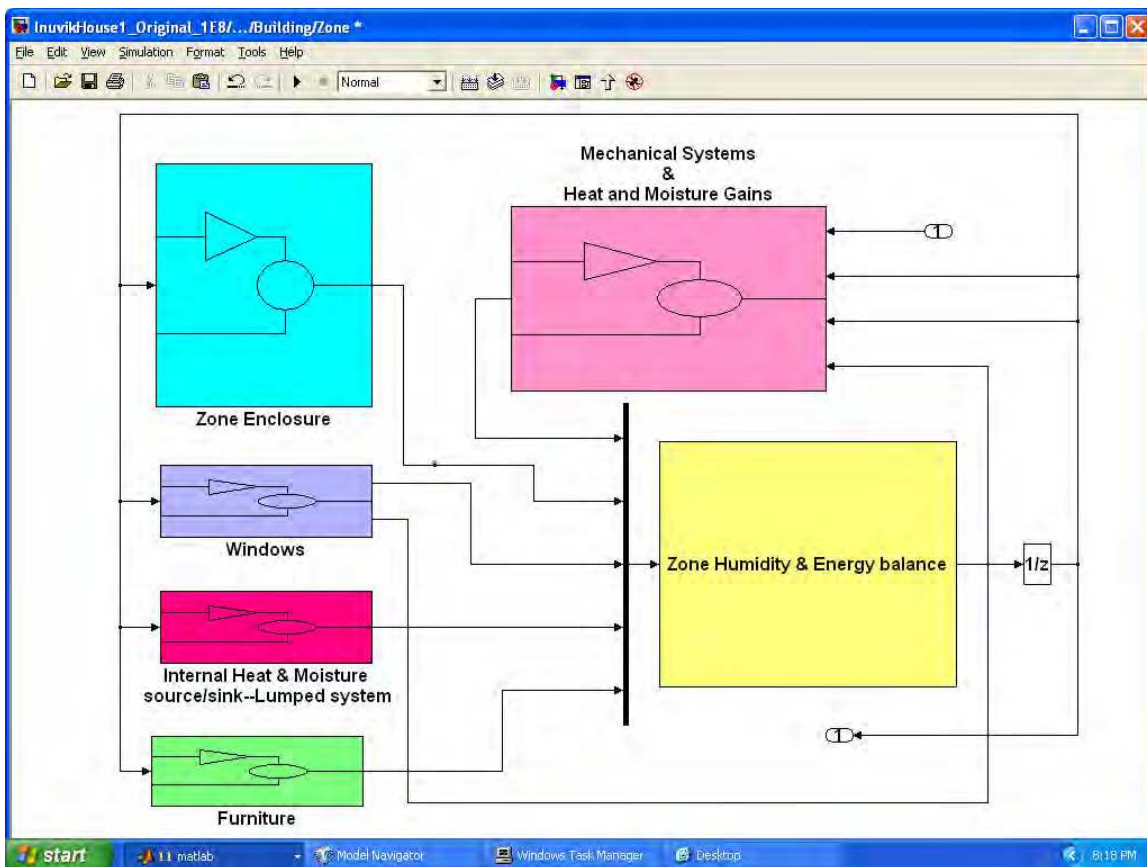


Figure 3 Virtual building as represented in the whole building hygrothermal model

3 BENCHMARKING OF THE WHOLE BUILDING HYGROTHERMAL MODEL

To evaluate the robustness and accuracy of a numerical model, Judkoff and Neymark [21] recommended three classes of tests be conducted namely: analytical verifications; comparison with other models, and; validations with experimental results. Accordingly, the whole building hygrothermal model was benchmarked against internationally published test cases that cover the three test categories. The newly developed hygrothermal model is referred as “HAMFitPlus” in the presentation and discussion of results.

3.1 Analytical verification

An analytical verification of the whole building hygrothermal model, HAMFitPlus, is carried out using test cases for which analytical solutions are available. The test case was originally formulated in the IEA⁵/Annex 41 project [22,23] and later published by Rode et al [24]. In this exercise, the quasi-steady indoor humidity condition of the simplified building, shown in Figure 4, is calculated. The whole building components (i.e. walls, roof and floor) are constructed from a monolithic layer of 150 mm thick aerated concrete. The material properties of the aerated concrete, represented in a simplistic manner, are given in Table 1. The external surfaces of all building envelope components (walls, roof and floor) are covered with a vapour tight membrane to avoid vapour loss from inside to outside. However, the interior surfaces of all building envelope components are open, where moisture exchange between indoor air and building enclosure is possible (Figure 5). The mass transfer coefficient for the interior surfaces is $2E-8$

⁵ IEA International Energy Agency

m/s. Furthermore, the following assumptions are made: 1) the initial conditions (temperature and relative humidity) of the building envelope components (walls, roof and floor) and indoor air are at 20°C and 30%, respectively; 2) the outdoor temperature and relative humidity are also constant and have the same values as the initial conditions; 3) the indoor temperature is held constant at 20°C during the simulation period, which results in isothermal moisture absorption and desorption processes; 4) the building is assumed to operate with a constant ventilation rate of 0.5 ACH (air-exchange per hour), and 500 g/hr indoor moisture gain during the time between 9:00 to 17:00 h.

The schematic diagram of the diurnal moisture production schedule is shown in Figure 6. The complete description of the exercises is given in Ruut and Rode [22]. For this test case, derivation of analytical solution is possible due to the various simplifying assumptions made in respect to the building geometry, boundary conditions, hygrothermal material properties, and also building operation.

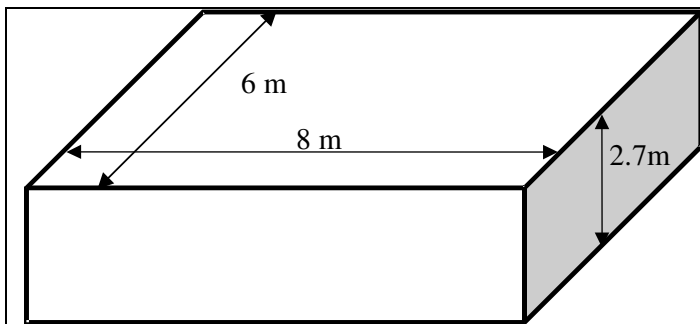


Figure 4 Schematic diagram of simplified building

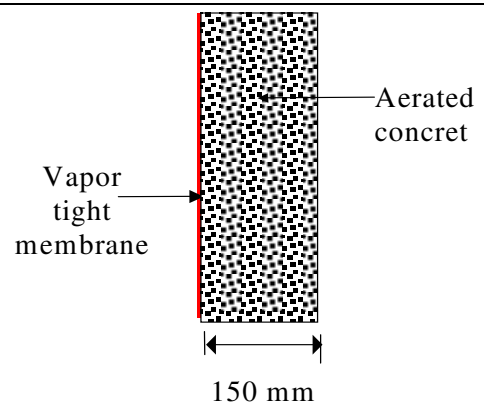


Figure 5 Typical building envelope component.

Table 1 Simplified material properties of aerated concrete

Thickness (m)	Density (kg/m ³)	Conductivity (W/mK)	Heat capacity (J/kgK)	Water vapour permeability (kg/m.s.Pa)	Sorption curve (kg/m ³)
0.15	650	0.18	840	3E-11	$w = 42.965\phi$

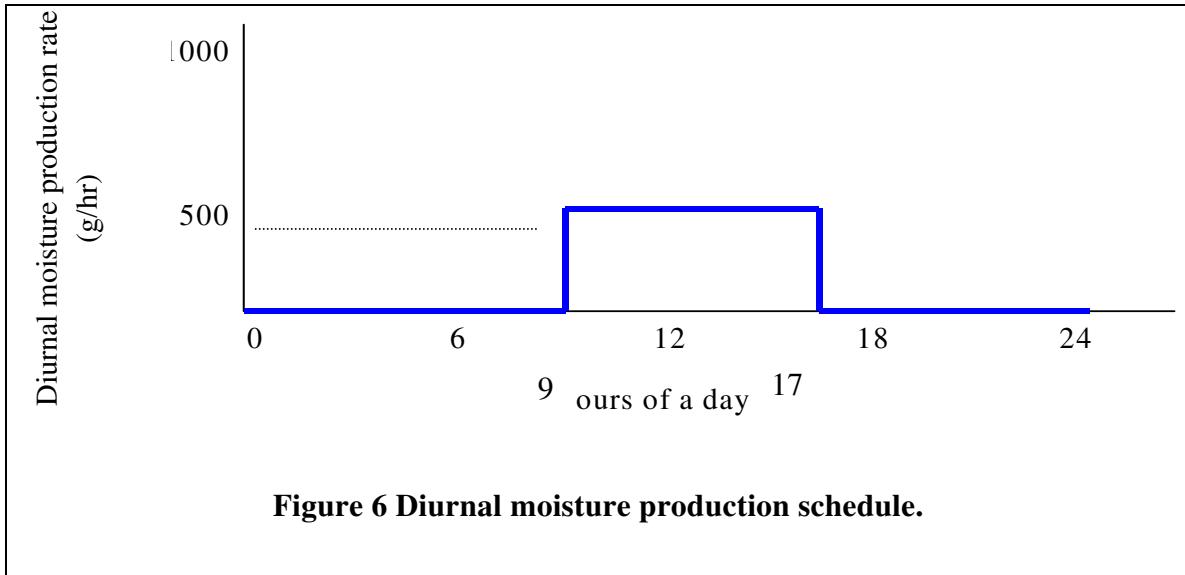
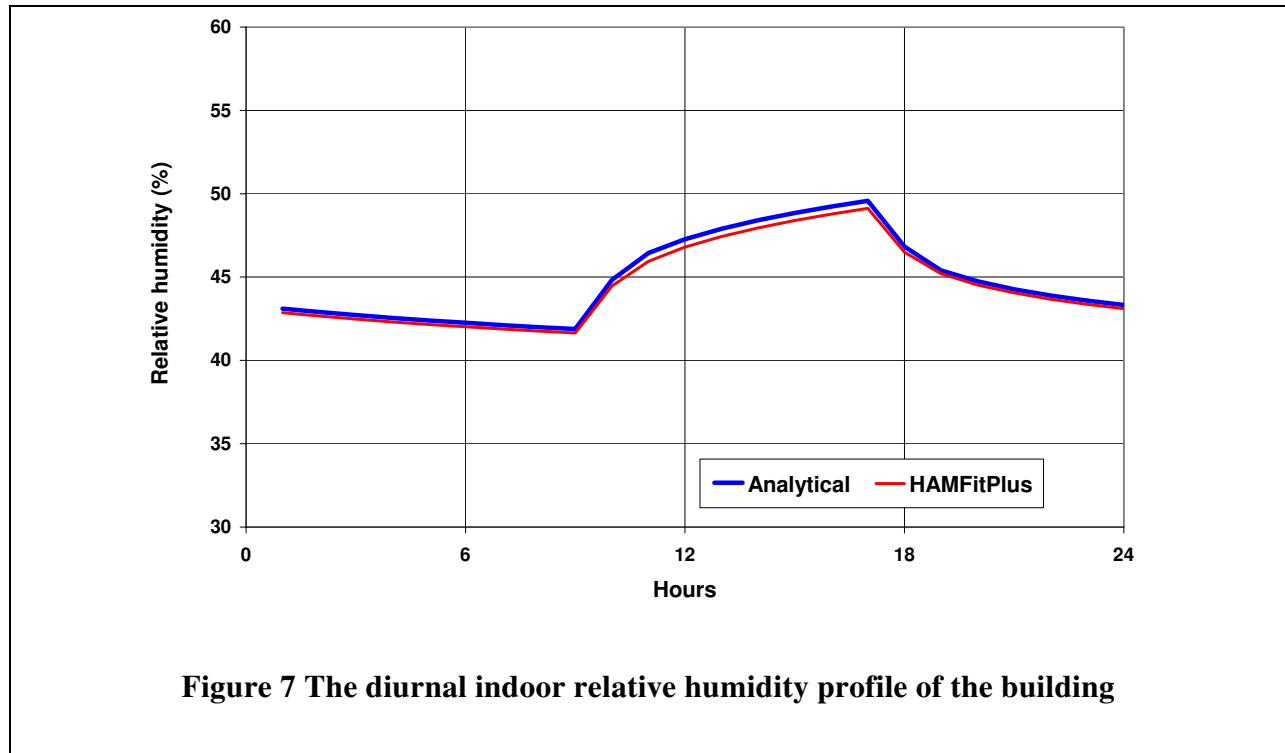


Figure 7 shows the hourly average relative humidity of the indoor air after a quasi-steady state condition is reached. The numerical prediction of HAMFitPlus is in excellent agreement with the analytical solution provided by Bednar and Hagentoft [25]. The indoor relative humidity steadily increases from 41.5% to 49% during the moisture generation period (9:00-17:00 h), and then decreases and completes the cycle (reduced to 41.5%), which is due to the presence of ventilation (0.5 ACH) and absence of moisture generation.



3.2 Comparative test

In this benchmark exercise [24] an integrated analysis of energy, indoor humidity and building envelope moisture conditions is carried out for a building exposed to the real weather condition of Copenhagen, Denmark (Altitude 5, longitude 12° 40' and latitude 55° 37'). The schematic diagram of the building considered for the whole building energy analysis is shown in Figure 8. The building is made of monolithic aerated concrete panels and has two south facing windows subjected to solar gain. The hygrothermal properties of the aerated concrete are taken from the IEA Annex 24 report [26]. The initial conditions of the construction and indoor air are 20°C and 80% relative humidity. The building envelope components can exchange moisture with both outdoor and indoor air as these surfaces are open for vapour transport. Subsequently, the dynamic moisture buffering effects of these components can influence the indoor humidity

condition of the building. The heat and mass transfer coefficients of the interior surfaces are $8.3 \text{ W}/(\text{m}^2 \text{ K})$ and $2\text{E-}8 \text{ kg}/(\text{s m}^2 \text{ Pa})$, respectively; the respective transfer coefficients for the exterior surfaces are $29.3 \text{ W}/(\text{m}^2 \text{ K})$ and $6.25\text{E-}8 \text{ kg}/(\text{s m}^2 \text{ Pa})$, respectively. These heat transfer coefficients represent the combined coefficients of heat transfer by convection and long-wave radiation heat exchange. The emissivity and absorptivity of the external opaque surfaces for long-wave and short wave radiations are 0.9 and 0.6, respectively. The windows have a U-value of $3 \text{ W}/\text{m}^2\text{K}$ and solar heat gain coefficient of one. The building is assumed to operate with a constant ventilation rate of 0.5 ACH (air-exchange per hour) and convective sensible heat and moisture gains of 800 W and 500 g/hr, respectively. These indoor heat and moisture generations are at constant rate and occurs between 9:00 h and 17:00 h similar to the schedule shown in Figure 6. The indoor temperature is maintained between 20 and 27°C using a thermostatically controlled mechanical system. The mechanical system is a 100% convective air system having infinite sensible heating and cooling, but zero latent heat capacities. The system provides heating if the air temperature is less than 20°C , and cooling if the air temperature is above 27°C . The indoor air temperature governs the operation of the thermostat.

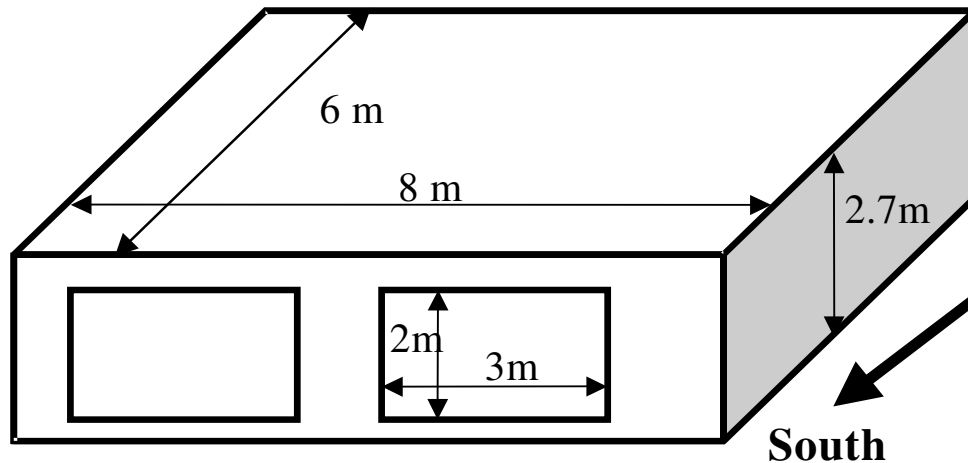


Figure 8 Schematic diagram of a building that is considered for whole building heat and moisture analysis

Simulation results

This test case involves interaction of the indoor environment, building envelope and HVAC systems. Based on the integrated analysis of these components, the heat and moisture conditions of the building on a typical day (July 5th) with the operational conditions specified above are presented in Figure 9. The simulation results of HAMFitPlus are shown in red, and that of all other models results are shown in gray curves. The parameters that are used for inter-model comparison cover the three aspects of whole building performance assessment. These are: 1) indoor environment: prediction of indoor temperature and relative humidity; 2) building envelope hygrothermal condition, viz. temperature and relative humidity conditions of the exterior surface of the roof; 3) energy consumption, viz. estimation of the heating and cooling loads that are required to maintain the indoor temperature in the desired range.

HAMFitPlus generates all these outputs simultaneously. In this comparative test, the HAMFitPlus simulation results of the indoor humidity and temperature conditions, hygrothermal conditions of the exterior roof surface and energy demands to maintain the desired indoor temperature are all well within the range of results obtained from the other models. In fact, the HAMFitPlus model is in close agreement with the batch of models whose solutions are close to one another.

HAMFitPlus simulation results for this typical day, indicate that: 1) The indoor relative humidity fluctuation by about 11%, with minimum and maximum values of 44 and 55%, respectively; 2) The roof surface temperature fluctuates as low as 12°C, during nighttime, and as high as 39°C at 13:00 h when the solar radiation is maximum. This temperature fluctuation can dictate the direction of moisture flow (solar driven moisture flow), and subsequently result in cyclic moisture condensation and evaporation in the roof structure. The highest moisture accumulation (corresponding to 76% relative humidity) is observed at the time when the roof surface temperature is the lowest; 3) The building requires heating from 1:00 to 9:00 h and cooling from 10:00 to 21:00 h. The hourly peak heating and cooling demands for that day are 1.16 and 5.68 kW, respectively. These energy demands occur at 5:00 and 14:00 h, respectively. Moreover, the annual heating and cooling loads are estimated to be 15420 and 1880 kWh, respectively.

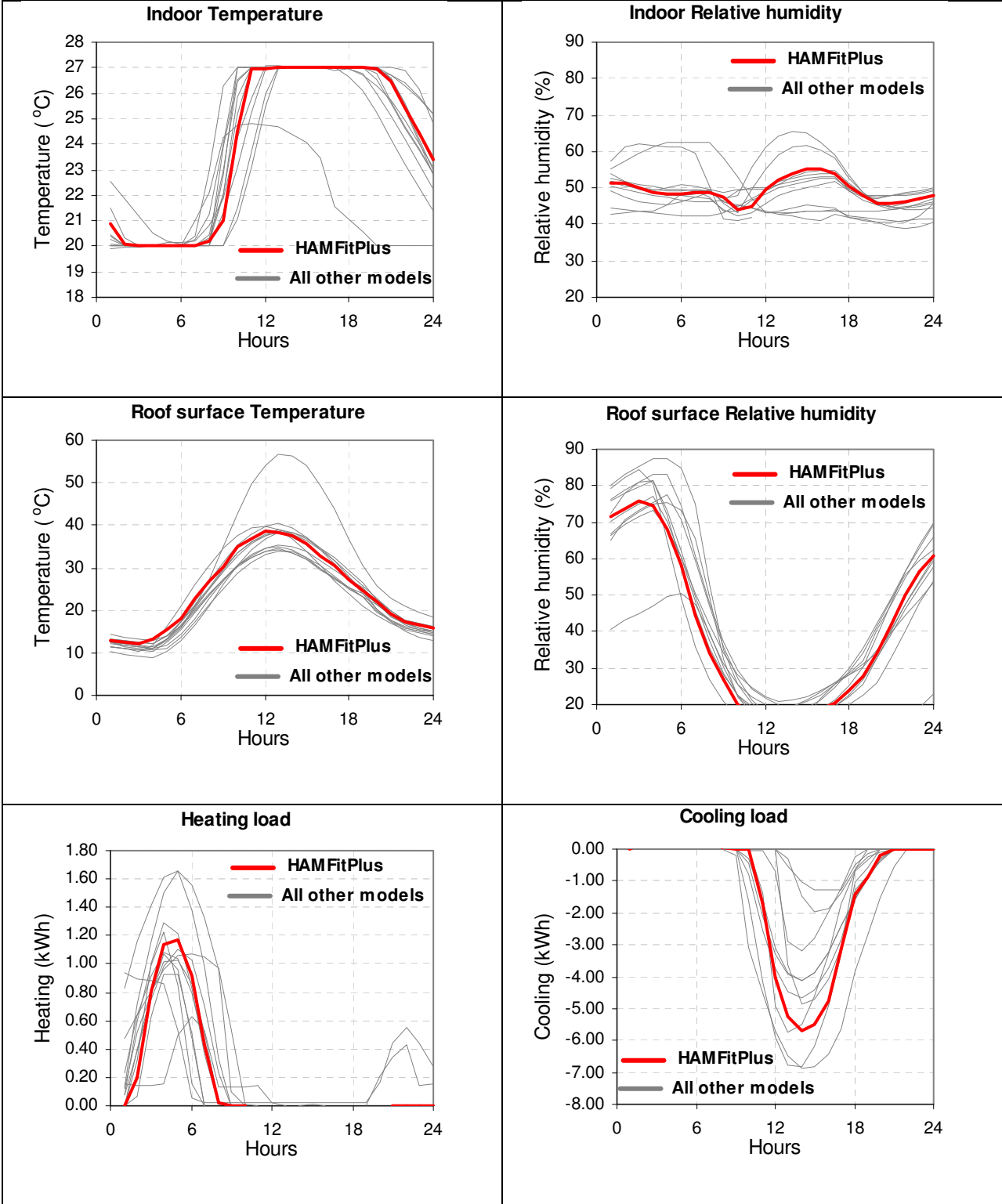


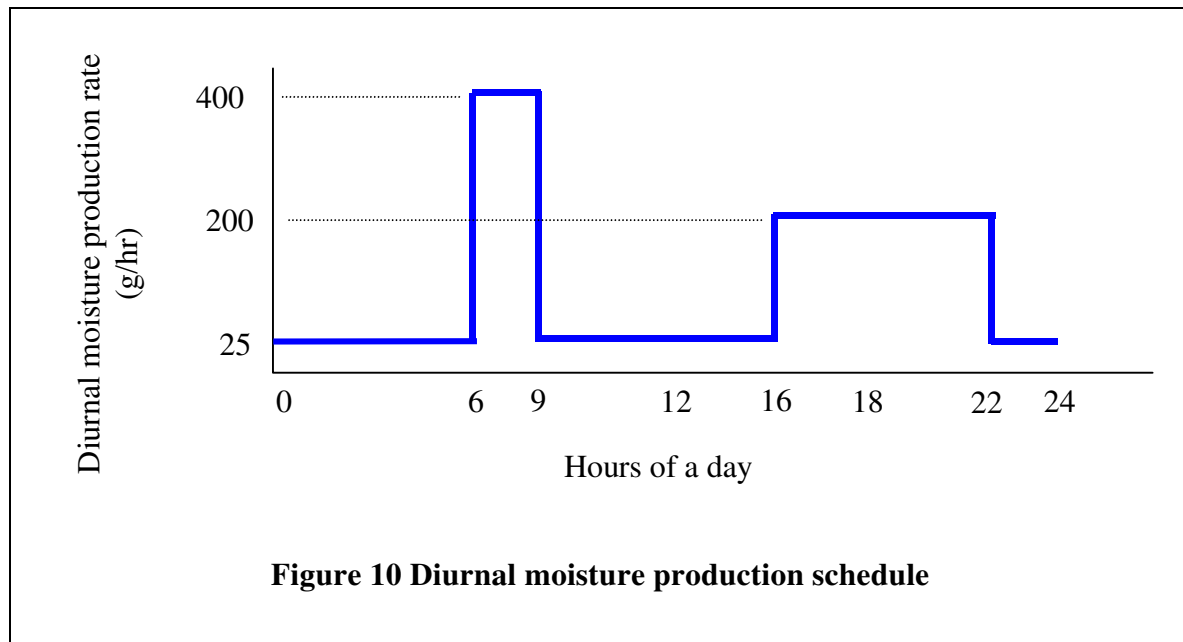
Figure 9 Integrated analysis results of indoor air, roof and energy demand of the building on July 5th.

3.3 Experimental validation—Two rooms with real climatic exposure

In this section HAMFitPlus is benchmarked with the field experimental data that is published in Holm and Lengsfeld [27]. In this experiment, two rooms that have identical geometry, dimensions, and orientation as well as boundary conditions are considered. Each room has a floor area of 19.34 m^2 and volume of 48.49 m^3 . One of the rooms is designated as a reference room and the other one as a test room. Their difference lies in the moisture buffering capacity of the interior finishing layers. The reference room walls and ceiling are painted with latex paint. The interior surfaces of the test room are unpainted, whereas the ceiling is covered with aluminum foil. The approximate vapor diffusion thickness of latex paint and aluminum foil are 0.15 m and 10000 m , respectively. The exterior surfaces of the reference and test rooms are exposed to real weather conditions of Holzkirchen, Germany. Holzkirchen is located at 47.88° north latitude and 11.73° east longitude, and has an elevation of 600 m . The temperature and relative humidity conditions of adjacent spaces are used as the boundary conditions of the respective surfaces. The ground temperature is assumed to be 2°C . The emissivity and absorptivity of the exterior and interior surfaces of the building components are 0.9 and 0.4 , respectively. A heat transfer coefficient of $8 \text{ W}/(\text{m}^2\text{K})$ is used for both internal and external surfaces of the partition walls, ceiling and hallway walls as well as the internal surfaces of the exterior walls and floor. The exterior surface heat transfer coefficient of the exterior walls is $18 \text{ W}/\text{m}^2\text{K}$. The thermal resistance between the exterior surface of the floor and the ground is assumed to be negligible, and represented in the model by high heat transfer coefficient ($100 \text{ W}/\text{m}^2\text{K}$)

3.3.1 Rooms operating conditions

During the experiment, the indoor temperatures of the two rooms are maintained at $20 \pm 0.2^\circ\text{C}$ using thermostatically controlled radiator heaters. The reported air exchange rates per hour due to both infiltration and mechanical ventilation system are 0.63 and 0.68 for the reference and test rooms, respectively. The rooms are subjected to identical indoor moisture load of 2.4 kg per day. The moisture load is distributed according to the diurnal moisture production schedule shown in Figure 10. According to this schedule, the occupants' morning activities (such as taking a shower) generates a peak moisture production rate of 400 g/hr for two hours (6:00-8:00 h). Whereas, their evening activities (such as cooking and washing dishes) result in a moderate moisture production rate of 200 g/hr for six hours (16:00-22:00 h). For the rest of the day a 25 g/hr moisture production rate, which represents moisture generation by other than the occupants' activity (such as pets or plants), is assumed.



3.3.2 Comparison of simulation and measured results

In this model validation exercise, HAMFitPlus predicts the indoor relative humidity conditions of the two rooms that have varying moisture buffering capacity and thereby different degrees of dynamic interaction between building envelope components and indoor air.

Figure 11 shows the indoor relative humidity of the two rooms for the measurement period of February 14 to March 20 2005 along with HAMFitPlus simulation results. The indoor humidity profiles of the respective rooms on a typical day, in this case February 17th, are presented in Figure 12. As can be seen in these figures, the simulation results of HAMFitPlus are in good agreement with the corresponding measured data. The good simulation results obtained here are attributed to the model's capability of handling the dynamic indoor air and building envelope heat and moisture interactions. The experimental and simulation results demonstrate the significance of moisture buffering materials in modulating and reducing indoor humidity fluctuation of a building. Generally, the indoor relative humidity amplitude of the test room is relatively smaller than that of the reference room. For example, the maximum and minimum indoor relative humidity of the reference room, which has a limited moisture buffering capacity, on February 17th are 57 and 24%, respectively (Figure 12). Whereas in the case of the test room, that has a higher moisture buffering capacity, the corresponding values are 47 and 27%, respectively (Figure 12). Consequently, the indoor relative humidity amplitudes of the two respective rooms are 33 to 20%. These results suggest that materials with high moisture buffering capacity provide a more stable indoor humidity condition (low fluctuation amplitude).

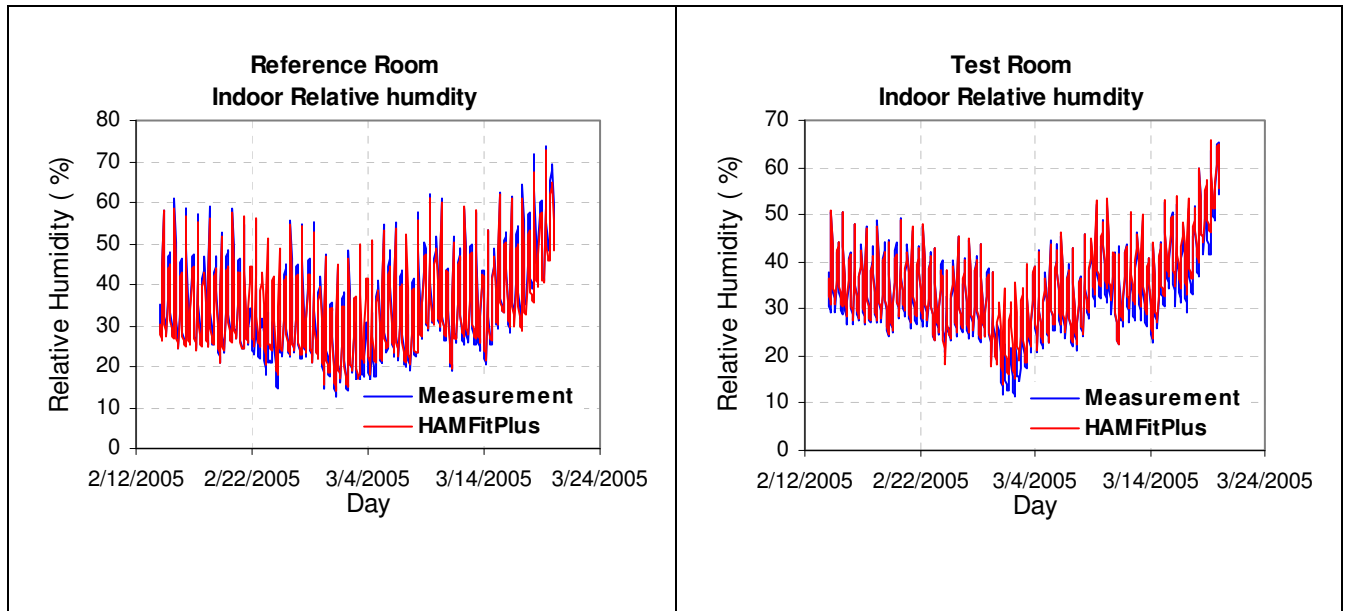


Figure 11 Measured and simulated indoor humidity of the Reference and Test rooms

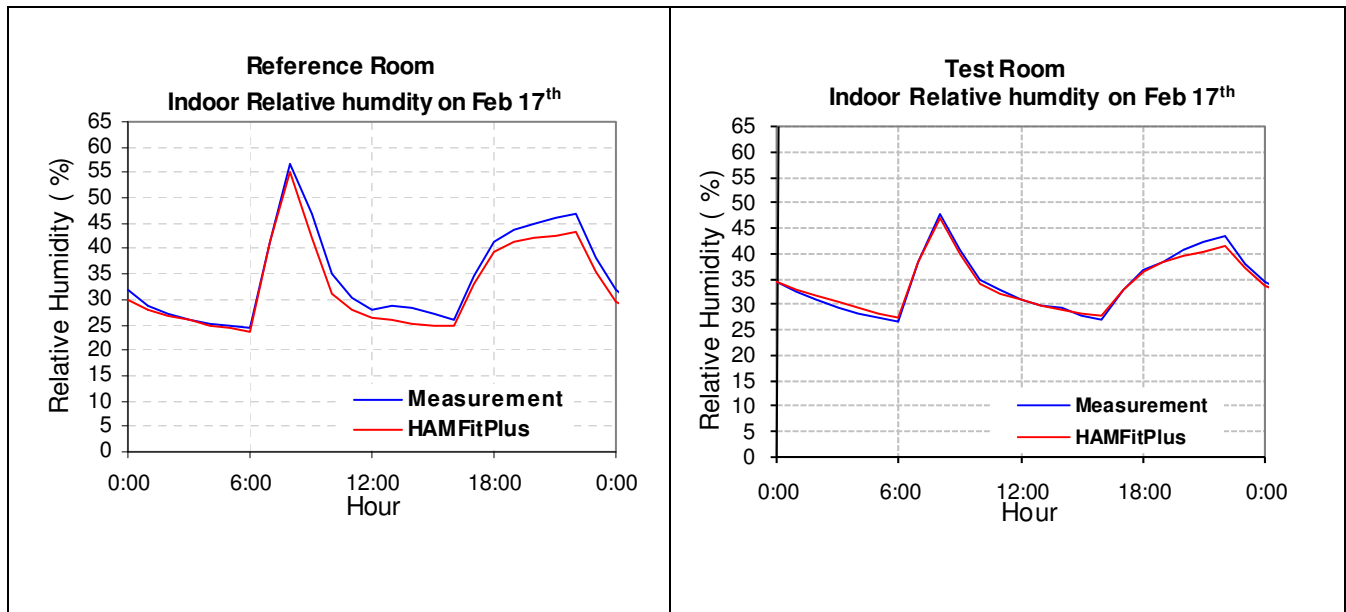


Figure 12 Measured and simulated indoor humidity of the Reference and Test rooms on February 17th

4 CONCLUSIONS

The three aspects of building design: durability, indoor condition, and energy performance, are interrelated. These three building performance parameters have to be considered simultaneously for optimized building design. Otherwise, there will be ambiguity of indoor boundary conditions in building envelope performance assessment; lack of information on moisture source and moisture buffering effects of interior materials in indoor humidity predictions; and inaccurate estimation of energy consumption and ventilation rates.

In this paper, a holistic HAM model is presented by developing and integrating building envelope and indoor models. The model is benchmarked against internationally published test cases that are comprised of analytical verifications, comparison with other models and validations with experimental results. As demonstrated in the benchmark exercises, the integrated model handles the dynamic heat and moisture interactions between building enclosure, indoor air and HVAC systems. The model can be further developed to a multi-zone whole-building HAM model by integrating it with a multi-zone airflow model. The whole building heat and moisture analyses that are presented in the paper underlines the importance of coupling building envelope and indoor environment to accurately predict the indoor humidity, energy consumption and durability of a building. Furthermore, the experimental and simulation results demonstrate the significance of moisture buffering materials in modulating and reducing the indoor humidity level of a building. The whole building hygrothermal model that is presented in this paper, HAMFitPlus, has already been applied in real case scenarios. The results in comparison with measured data will be presented in future publications.

5 REFERENCES

- [1] Shaw, C.Y. and Kim, A. (1984). Performance of Passive Ventilation Systems in a Two-Store House, *5th AIC conference*, October 1-4, Reno, Nevada, USA.
- [2] TenWolde, A. (1988). Mathematical Model for Indoor Humidity in Houses during Winter, Proceedings of Symposium on Air Infiltration, Ventilation and Moisture Transfer, Washington DC: Building Thermal Envelope Coordinating Council.
- [3] Loudon, A.G. (1971). The Effect of Ventilation and Building Design Factors on the Risk of Condensation and Mould Growth in Dwellings. *The Architects' Journal*, Vol. 153 (20), pp. 1149-1159.
- [4] Hutcheon, N.; Handegord, G. (1995). Chapter 12: Water and Buildings, *Building Science for a Cold Climate*, National Research Council of Canada.
- [5] Tsongas, G.; Burch, D.; Roos, C.; Cunningham, M. (1996). A Parametric Study of Wall Moisture Contents Using a Revised Variable Indoor Relative Humidity Version of the MOIST Transient Heat and Moisture Transfer Model. Proceedings of the Thermal Performance of Exterior Envelopes VI Conference, Dec. 4-8, Clearwater Beach, FL.
- [6] TenWolde, A. (2001). Interior Moisture Design Loads for Residences. *Building VIII: Performance of exterior envelopes of whole buildings*. Dec. 2-7, Clearwater, FL.
- [7] El Diasty, R.; Fazio, P.; Budaiwi, I. (1992). Modelling of Indoor Air Humidity: The Dynamic Behaviour within Enclosure. *Energy and Buildings*, Vol. 19, pp.61-73.
- [8] Jones, R. (1993). Modeling Water Vapor Conditions in Buildings. *Building Services Engineering Research and Technology*, Vol. 14 (3), pp.99-106.

- [9] Christian, J.E. (1994). Moisture Sources. Moisture Control in Buildings, ASTM Manual Series: MNL 18, pp. 176-182.
- [10] Tariku, F.; Cornick, S.; Lacasse, M. (2007). Simulation of Wind-Driven Rain Effects on the Performance of a Stucco-Clad Wall. Proceedings of Thermal Performance of the Exterior Envelopes of Whole Buildings X International Conference. Dec. 2-7, Clearwater, FL
- [11] Tariku, F.; Kumaran, M. K. (2006). Hygrothermal Modeling of Aerated Concrete Wall and Comparison With Field Experiment. Proceedings of the 3rd International Building Physics /Engineering Conference, August 26-31, Montreal, Canada, pp 321-328.
- [12] Kuenzel, H.M. (1995). Simultaneous Heat and Moisture Transport in Building Components: One- and Two- dimensional calculation using simple parameters, PhD. Thesis, University of Stuttgart, Germany.
- [13] Burch, D. M. (1993). An Analysis of Moisture Accumulation in Walls Subjected to Hot and Humid Climates. ASHRAE Transactions, Vol. 99, Part 2.
- [14] Pederson, C. R. (1990). Combined Heat and Moisture Transfer in Building Constructions, Ph.D. Thesis, Report no. 214, Thermal Insulation Laboratory, Technical University of Denmark.
- [15] Mendes, N.; Winkelmann, F.C.; Lamberts, R.; Philippi, P.C. (2003). Moisture Effects on Conduction Loads, Energy and Buildings, Vol. 35, pp. 631-644.
- [16] Tariku, F.; Kumaran, K.; Fazio, P. (2010). Transient Model for Coupled Heat, Air and Moisture Transfer through Multilayered Porous Media. Accepted for publication in the International Journal of Heat and Mass Transfer.
- [17] Tariku, F. (2008). Whole Building Heat and Moisture Analysis. Ph.D. Thesis. Concordia University, Montreal, Canada.

- [18] Henderson, H., and K. Rengarajan. (1996). A model to predict the latent capacity of air conditioners and heat pumps at part- load conditions with constant fan operation. ASHRAE Transactions 102(1): 266-274.
- [19] Shirey, D.B., H.I. Henderson and R. Raustad. (2006). Understanding the Dehumidification Performance of Air-Conditioning Equipment at Part-Load Conditions. Final Report FSEC CR-1537-0. DOE/NETL Project No. DE-FC26-01NT41253.
- [20] European Standard prEN ISO 13791 (2004). Thermal Performance of Buildings Calculation of Internal Temperatures of a Room in Summer Without Mechanical Cooling General Criteria and Validation Procedures. ISO/FDIS 13791:2004.
- [21] Judkoff, R.; Neymark, J. (1995). Building Energy Simulation Test (BESTEST) and Diagnostic Method. NREL/TP-472-6231. Golden, CO National Renewable Energy Lab.
- [22] Ruut P.; Rode, C. (2004). Common Exercise 1 – Case 0A and 0B Revised. IEA, Annex 41, Task 1, Modeling common exercise.
- [23] Ruut P.; Rode, C. (2005). Common Exercise 1 “Realistic” Case. IEA, Annex 41, Task 1, Modeling common exercise.
- [24] Rode, C.; Ruut, P.; Woloszyn, M. (2006). Simulation Tests in whole Building Heat and Moisture Transfer, Proceeding of the 3rd International Building Physics /Engineering Conference, August 26-31, Montreal, Canada, pp 527-534
- [25] Bednar, T.; Hagentoft, C. (2005). Analytical Solution for Moisture Buffering Effect Validation Exercises for Simulation Tools. *Nordic Building Physics Symposium*, Reykjavik, June 13-15.

- [26] Kumaran, M.K. (1996). Heat, Air and Moisture Transfer through New and Retrofitted Insulated Envelope Parts, IEA Annex 24 HAMTIE, Final Report, Vol.3, Task 3: Material Properties.
- [27] Holm, A.; Lengsfeld, K. (2007). Moisture-Buffering Effect—Experimental Investigations and Validation. Proceedings of Thermal Performance of the Exterior Envelopes of Whole Buildings X International Conference. Dec. 2-7, Clearwater, FL.